ELSEVIER

Journal of Structural Geology 28 (2006) 1307–1315

JOURNAL OF STRUCTURAL GEOLOGY

www.elsevier.com/locate/jsg

Scaling properties of thrust fault traces in the Himalayas and inferences on thrust fault growth

Sumit Kumar Ray *,[1]

Geological Survey of India, Central Headquarters (PPM Div), 27 J L Nehru Road, Kolkata 700 016, India

Received 14 February 2005; received in revised form 22 February 2006; accepted 23 February 2006
Available online 4 May 2006

Abstract

Map traces of thrust faults in the Himalaya show a conspicuous cuspate–lobate pattern, i.e. broad lobes joined by sharp angular cusps. For each lobe, we can draw a chord by joining the apices of two adjacent cusps, and define amplitude (A) by perpendicular distance of apex of the lobe from its chord. The lobes show a linear scaling defined by the relationship $A = cL$, where L is the chord length and c is a constant. The L/A ratio remains nearly constant over about 1.71 orders of magnitude spread of the L values of the sampled lobes, suggesting that A is proportional to L. The trace pattern indicates that the thrust surfaces are laterally curved due to the growth of fault segments from multiple nuclei, along concave-upward laterally curved trajectories. The propagating surfaces coalesce along sharp angular ridges. This lateral curvature gives a furrow-like shape to each segment, and a fluted appearance to the thrust surfaces. The invariant nature of the L/A ratio supports self-similarity and is manifest as a linear scaling of A against L of the lobes. The self-similarity further suggests the possibility of thrust fault growth along a characteristic curved surface.

Keywords: Fault scaling; Thrust fault; Fault trace; Fault growth; Himalaya

1. Introduction

Traces of thrust faults in fold-and-thrust belts are generally sinuous. Examination of published geological maps of the Himalaya (Fig. 1) reveals that although traces of the major thrust faults, which have controlled map patterns of the Lesser Himalaya, have a general east–west trend parallel to the mountain front, in detail they show a sinuous pattern. The thrust traces are cuspate–lobate, with broad lobes, convex towards the foreland, joined by sharp reentrants, which define the cusps pointing towards the hinterland (Fig. 1). Geometrical analysis presented in this paper examines the scaling relationships and significance of the cuspate–lobate shapes.

Traces of gently to moderately dipping thrust surfaces may be conspicuously sinuous in areas of rugged topography. Deep river valleys carve out sharp cuspate features separating broad lobes on thrust traces. The amplitude of such cusps or lobes depends on the depth of the valleys and dip of the thrust surfaces. The traces of folded thrust surfaces may be sinuous. Besides topographic effects and post-thrusting warping, different researchers have cited differential thrust transport (e.g. Elliott, 1976; Macedo and Marshak, 1999), or thrust fault growth along laterally curved trajectories (e.g. Ray, 1995) as the factors that give rise to curved thrust traces. The present paper assesses whether these factors separately or in combination explain the observed cuspate–lobate trace pattern (Fig. 1) and the observed scaling relationship. The significance of this pattern in understanding fault growth is also discussed.

2. Fault trace patterns—map analysis

In common with many other thrust belts, thrust traces in the Lesser Himalaya are not irregular curves but follow a regular geometric pattern. For example, the map traces of the Shumar thrust in the eastern sector of the Bhutan Himalaya (Fig. 1a), the Main Central Thrust (MCT) in the Garhwal–Kumaon sector (Fig. 1b, c and e) of the Uttaranchal Himalaya and the Kulu–Rampur sector (Fig. 1d) of the Himachal Himalaya all show cuspate–lobate patterns. The map of the Nepal Himalaya (Fig. 1f) reveals a multiple-lobate pattern that is a characteristic and consistent feature of all the thrusts mapped by Kizaki et al. (1982). Moreover, the larger lobes are often further divisible into several smaller lobes. Such sub-lobes, however, are less prominent in the examples of maps from other parts of the

* Tel.: +91 33 2286 1693; Fax: +91 33 2286 1656.
E-mail address: skray45@yahoo.co.in.
[1] Present address: Centre for Studies of Man and Environment, CK-11 Salt Lake, Sector-II, Kolkata 700 091, India. Tel: +91 33 30120781. Fax: +91 33 30120781.

0191-8141/$ - see front matter © 2006 Elsevier Ltd. All rights reserved.
doi:10.1016/j.jsg.2006.02.010

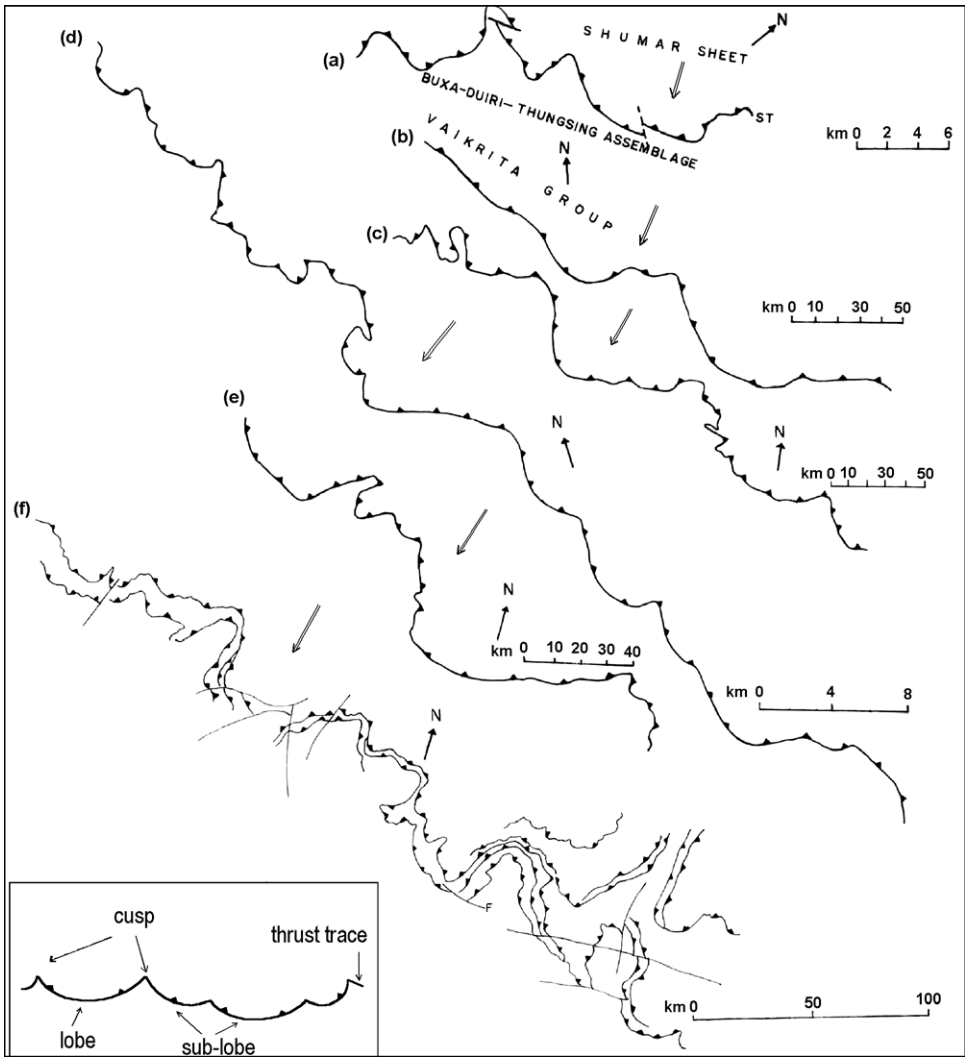

Fig. 1. Segments of thrust traces mapped by different workers in different sectors of the Himalaya. The teeth indicate the hanging walls and dip direction of the thrust surfaces. (a) The Shumar thrust, Bhutan Himalaya (Ray et al., 1989; Ray, 1995). (b) The Main Central Thrust (MCT) of the Garhwal–Kumaun sector, Uttaranchal (Jangpangi, 1982). (c) The MCT in the Garhwal–Kumaun sector, and eastern Himachal Pradesh (Ahmad, 1979). (d) The Jutogh/Kulu thrust, Kulu–Rampur sector, Himachal Pradesh, (Sharma, 1977). (e) The MCT in the area towards the west of the thrust shown in (b) (Sharma and Virdi, 1982). (f) Regional scale thrusts of central east Nepal (Kizaki et al., 1982). The map traces show a cuspate–lobate pattern (see text) with broad lobes convex towards south, i.e. towards the foreland. The sharp cusps point towards the hinterland of the fold-and-thrust belt. All the thrust surfaces dip towards the hinterland. The inset shows a sketch of gently curved lobes and sub-lobes, and sharp angular cusps of the cuspate–lobate trace pattern. The arrows with 'N' at arrowheads indicate the north direction of the map traces. The other set of arrows gives the thrust transport direction.

Himalaya that are cited in this paper. On hinterland dipping thrusts, the lobes are convex towards the foreland, and joined by sharp angular projections or cusps pointing towards the hinterland.

The geometry of the lobes can be described using chord length (L) and amplitude (A), as defined in Fig. 2. End-points (E) and apices (P), separated by limbs (l) of the sampled lobes were marked on tracings of the printed regional maps, and the L and A values were measured. Chord length (L) and amplitude (A) values for the major lobes on sampled segments of the thrust fault traces are given in columns 2 and 3 of Table 1.

Table 1 shows that amplitude (A) increases with chord length (L). The L values of the sampled lobes range from 3.37 to 200 km, i.e. 1.71 orders of magnitude, whereas the L/A ratios (Table 1) range only 0.66 orders of magnitude, from 1.3 to 5.94. This comparatively narrow range of the L/A ratios, in spite of the variable topographic effects and the likely inaccuracies and approximations in determination of L and A from the printed source maps, suggests that the L/A ratio is nearly constant. The L vs. A plot (Fig. 3) illustrates this linear scaling relationship. The topographic effects, which have contributed to the sinuosity of the traces, vary from lobe to lobe. An invariant L/A ratio indicates that the relationship between chord length and amplitude of the lobes on the map traces (Fig. 1) is of the form:

$$L = cA \tag{1}$$

where c is a constant equal to the slope of the best fit line in Fig. 3.

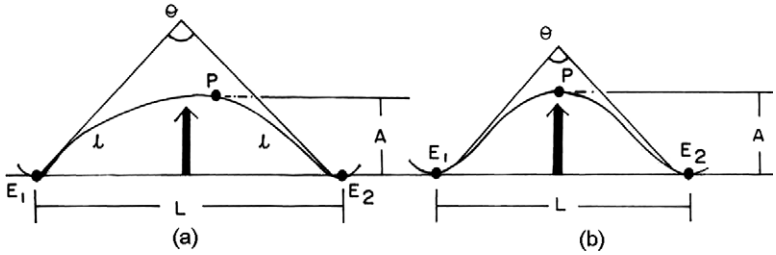

Fig. 2. The geometric elements of lobes on thrust fault traces. The terminology of fold-and-thrust belt salients of Macedo and Marshak (1999) has been adopted with modifications. E_1, E_2—end-points at which the lobe terminates. The end-points are the apices of the two adjacent cusps. P—apex, the point on the lobe where curvature is a maximum. *L*—chord length, the distance between the two end points. l—limb. *A*—amplitude, the distance between the chord and the apex of a lobe. θ—interlimb angle. (a) Asymmetric lobe. (b) Symmetric lobe, where the apex lies on the perpendicular bisector of the chord.

2.1. Scale invariant, self-similar character

The analysis presented in Figs. 1 and 3 and Table 1 is based on regional maps, of widely varying scales (Fig. 1) suggesting that the linear scaling property of the lobes in Fig. 1 is scale invariant. The map of the Nepal sector (Fig. 1f) shows sub-lobes within larger lobes. The *L* and *A* values of the sub-lobes have the same scaling relationship as that of the larger order lobes supporting a scale invariant relationship.

The size of the sampled lobes varies widely. Fig. 4a and b shows that on a reference frame defined by the chord length along the X-axis with the chord mid-point at the origin, the different symmetric arcs of a curve plot as a set of parallel curves. Such a parallelism indicates a kind of self-similarity, and implies that the arcs on varying chord lengths are segments of a particular curve. In Fig. 4c, the sampled lobes in Fig. 1 were plotted on a reference frame as defined above. The plot of the lobes yields a set of nearly parallel curves. The departure from perfect parallelism can be attributed to variable topographic effects, inaccuracies in determination of *L* and *A*, and variations in dip of the thrust faults. Fig. 4 thus provides supporting evidence of a self-similar geometry for the lobes and implies that the lobes are symmetric arcs of a particular curve.

Whether the cuspate–lobate pattern with the characteristic geometry and scaling relationship of the lobes can be explained by topographic effects, or folding of thrust surfaces, or differential transport, is now examined in the following sections.

3. Causes of curved thrust traces

3.1. Effect of topography

The topographic controls on the map trace patterns of gently dipping fault surfaces can be considerable. Fig. 5 shows how two transverse valleys with the valley axes sloping opposite to the dip of the fault surface produces a broad lobe between two 'V'-shaped cusps of the fault trace (Fig. 5a and b). Fig. 5c and d defines the relationship between *A* (amplitude = distance RR′), α (dip of the fault surface) and RO, which is the elevation difference (*h*) between the end points and the apex (P) of the lobe. It has been shown (Ray, 2000) that

$$\mathrm{RO} = A\tan\alpha \quad \text{or} \quad A = \mathrm{RO}/\tan\alpha \tag{2}$$

The relationship in Eq. (2) indicates that amplitude *A* depends on the dip of the fault plane (α) and elevation difference between the apex and end points of a lobe. If $\alpha = 30°$ and *A* is 30 km, the required elevation difference is 17.32 km. And for $\alpha = 15°$, it is 8.04 km. For steeper dips the required level difference will be correspondingly greater. The dips of the thrust surfaces shown in Fig. 1a–d are typically 30° or more (Sharma, 1977; Ahmad, 1979; Jangpangi, 1982; Ray et al., 1989). Table 1 shows that the amplitude of many of the lobes exceeds 10 km, which, if formed because of topographic effect only, require an elevation difference of >5.77 km between the apex and end points of the lobes (assuming a 30° dip of the thrust surface). The amplitude is more than 30 km in some of the lobes. The required elevation difference for a 30° dipping thrust surface is >17.32 km. Such elevations are not found anywhere: Mount Everest summit, the highest point on the Earth's surface, is approximately 9 km above sea level. Hence the amplitude range of the lobes in Fig. 1 cannot be accounted for solely as an effect of topographic cut and erosion. Uneven topography has therefore only contributed to some of the trace line curvatures.

The amplitude *A* of a lobe formed because of topographic effects will be $A = h/\tan\alpha$ (Fig. 5). A lobe of amplitude $(A) > h/\tan\alpha$ would indicate that in addition to the topographic effect, other factor(s) has/have contributed a component $[A - (h/\tan\alpha)]$ to the lobe amplitude. The topographic effect of each of the sampled lobes could not be separately estimated because the elevation data of the end-points and apices are not available in the source maps of the faults in Table 1.

The apices of cusps formed due to topographic effects should lie in valley bottoms. No such clear relationship in spatial distribution of the cusps and valleys is seen in the Himalayan examples shown in Fig. 1. In the Garhwal–Kumaun Himalaya, many prominent rivers like Bhilangana, Tons, Alaknanda (Sharma and Virdi, 1982), Bhagirathi, Yamuna (Ahmad, 1979), Pindar, Kali, Sarayu, and Mandakini (Jangpangi, 1982), flow across the lobes on the regional thrusts shown in Fig. 1b, c and e. Some of the cusps in the Kulu–Rampur sector, however, lie in valley bottoms (Sharma, 1977).

If formed due to topographic effects, the chord length of the lobes will depend on the separation between the valleys, because the end points of the lobes will lie in the valley

Table 1
Amplitude (*A*) and chord length (*L*) scaling relationship of the lobes on thrust fault traces from different sectors of the Himalayas

Sr. No.	Chord length (*L*) in km	Amplitude (*A*) in km	*L*/*A*	Thrust fault and sector	Location (longitude passing approximately through the middle of the sector)	Average dip of the thrust
1	2	3	4	5	6	7
1.	12.25	4.13	2.97	Shumar Thrust (Fig. 1a). East Bhutan sector	E 91° 30′	28° (Ray et al., 1989)
2.	6.00	2.95	2.03			
3.	8.00	3.25	2.46			
4.	97.33	25.33	3.84	The Main Central Thrust (MCT) (Fig. 1b). Garhwal–Kumaun sector, Uttaranchal	E 79° 30′	35° (Geological Survey of India, 1989, p. 92)
5.	15.33	2.67	5.74			
6.	53.32	13.33	4.00			
7.	89.30	22.80	3.92	The MCT (Fig. 1c). Garhwal–Kumaun–Himachal sector, Uttaranchal and Himachal Pradesh	E 79° 10′	35° (Geological Survey of India, 1989, p. 92)
8.	102.60	32.30	3.18			
9.	47.50	17.10	2.78			
10.	15.00	3.50	4.29	Jutogh/Kulu Thrust (Fig. 1d). Kulu–Rampur sector, Himachal Pradesh	E 77° 30′	30° (Sharma, 1977, pl. 3)
11.	6.25	1.69	3.70			
12.	5.87	1.06	5.53			
13.	11.50	4.13	2.79			
14.	10.00	2.88	3.48			
15.	3.92	1.63	2.41			
16.	90.00	33.53	2.68	The MCT (Fig. 1e). Garhwal–Kumaon sector, Uttaranchal	E 78° 45′	35° (Geological Survey of India, 1989, p. 92)
17.	12.94	3.53	3.67			
18.	64.71	15.29	4.23			
19.	17.65	3.53	5.00			
20.	12.95	9.42	1.375			
21.	32.20	11.65	2.76	Higher Himalayan thrusts (Fig. 1f). East Central Nepal	E 84°	–
22.	16.44	9.59	1.71			
23.	37.00	6.85	5.40			
24.	32.20	8.91	3.61			
25.	41.10	13.70	3.00			
26.	50.00	32.20	1.55			
27.	15.76	5.48	2.88			
28.	11.65	8.91	1.31			
29.	28.77	18.50	1.56			
30.	145.26	45.79	3.17	The Main Central Thrust, Arunachal Pradesh (Kumar, 1997)	E 94°15′	35° (Kumar, 1997, p. 97)
31.	175.13	43.78	4.00	The Main Boundary Thrust (MBT)/ Krol Thrust. Himachal Pradesh (Srikantia and Bhargava, 1998)	E 77°30′	35° (Srikantia and Bhargava, 1998, p. 162)
32.	60.00	10.54	5.69			
33.	120	24.71	4.86	The MBT/Krol thrust, Kashmir and Himachal Pradesh (Nanda and Mathur, 2000)	E 76°30′	35° (Srikantia and Bhargava, 1998)
34.	122.35	24.71	4.95			
35.	111.76	18.82	5.94			
36.	200.00	47.06	4.25			
37.	176.47	43.53	4.05			
38.	137.65	24.71	5.57			
39.	18.82	5.88	3.2			
40.	138.0	32.0	4.31	Main Boundary Fault, Himachal Pradesh. (Geological Survey of India, 1989)	E 77°30′	35° (Srikantia and Bhargava, 1998)
41.	196.0	64.0	3.06			

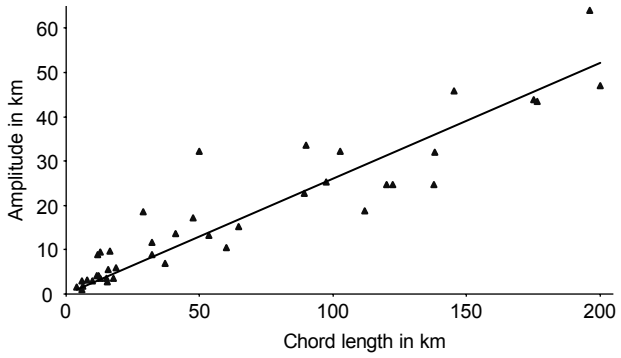

Fig. 3. Plot of amplitude (A) versus chord length (L) of the sampled lobes on the thrust traces in Table 1.

bottoms. Amplitude will then be controlled by depth and gradient of the valleys and dip of the thrust surfaces. As the separation between valleys is typically irregular, as is the profile of the valleys in the Himalaya (Seeber and Gornitz, 1983), the observed linear scaling relationship between L and A (Fig. 3) cannot be explained as an effect of topography.

3.2. Post-thrusting folding

A curved map trace on an even topographic surface suggests a curved thrust surface. A planar thrust surface may become curviplanar because of post-thrusting folding.

The traces of the sampled thrust segments are cuspate–lobate and not a train of antiforms and synforms as is expected during folding. Ramsay and Huber (1987, p. 397), however, postulated that folding of interfaces separating incompetent and competent layers, and oriented along a direction of shortening, will have alternating round and sharp crested folds, which they termed ‘cuspate–lobate folds’. They observed that folds formed by deflection of the more competent material into the less competent material would have a more rounded shape and larger wavelength compared with deflections of the less competent material into the more competent material, which would show sharp crests and smaller wavelength. Thrust surfaces that separate rocks with different competences in the hanging wall and footwall sheets could be deformed in an analogous way to form cuspate–obate folds. The map traces of such folded surfaces will have a cuspate–lobate shape resembling the trace pattern of thrust surfaces in Fig. 1. The following analysis, however, indicates that the cuspate–lobate pattern (Fig. 1) is not a result of folding.

(1) Folding of thrust surfaces to generate the observed trace pattern requires a significant component of shortening parallel to the thrust surface at high angles to the direction of orogenic convergence. Evidence of such a regional-scale east–west shortening is not present in the Himalaya. On the contrary, most workers have inferred extension (and extrusion) in the east–west direction based on the development of normal faults and oblique strike-slip faults (e.g. Armijo et al., 1986; Le Pichon et al., 1992).

(2) The lobes in Fig. 1 typically show deflection into the footwall blocks. If these features formed due to folding, the lobes would indicate that the rocks of the hanging wall are always more competent compared with the rocks of the footwall (cf. Ramsay and Huber, 1987). This may be true in the case of the MCT, where the high grade crystalline rocks and granitic gneisses constitute the hanging wall rocks. Elsewhere, however, the situation is different. The Shumar thrust sheet for example, (Fig. 1a; also Ray, 1991, fig. 5; Ray et al., 1989) is composed of phyllite—foliated quartzite—marble bands, and is thrust over massive dolomite–quartzite association of the Buxa thrust sheet, which is more competent.

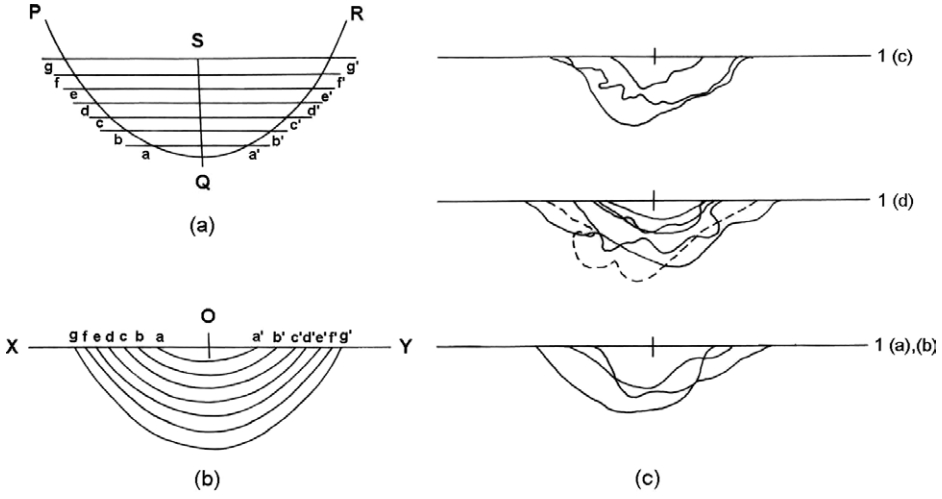

Fig. 4. Diagram to illustrate self-similar geometry of the lobes. (a) PQR is an arbitrarily drawn curve, symmetrical about the median line QS. a–a′, b–b′,…,g–g′ are chords of symmetrical arcs. (b) The chords a–a′, b–b′,…,g–g′, and their respective arcs are plotted on a common reference line X–Y, with the chord mid-points at the common point O. The arcs plot as a set of nearly parallel curves. (c) Some of the lobes in Fig. 1d and e and Fig. 1a and b, respectively, have been separately plotted on common reference lines and common chord mid-points. The lobes, irrespective of their map scales, plot as a set of nearly parallel curves. By analogy with (a) and (b), it may be suggested that the lobes are arcs with a particular curve.

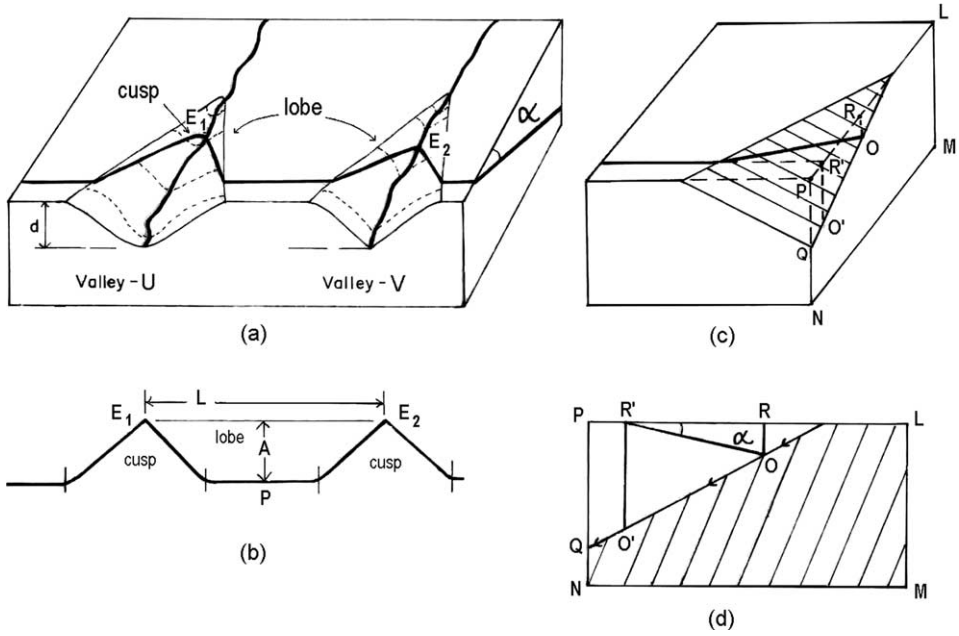

Fig. 5. Block diagram depicting the outcrop pattern formed because of two parallel valleys (valleys U and V) with the valley axes trending at high angles to the strike of a fault (the heavy dark line) and sloping opposite to the dip of the fault. d is the depth of the deepest part of the valley in the figure, α is dip of the fault plane. (b) The corresponding trace pattern of the fault is shown. The pattern may be described as cuspate–lobate if the sharp angles of the fault trace are smoothened, as is likely in natural situations. L, A, and E_1, E_2 are as defined in Fig. 2. (c) Block diagram, showing only one side-wall of a valley and the fault trace on the valley wall. LMNP is a vertical plane through the valley axis; R and R′ are projections of the end point and the apex respectively on the line PL. RR′ is equal to amplitude. (d). The LMNP surface, on which the fault trace has been projected to find the relationship between RR′, α, and RO (RR′ = RO/tan α).

It appears therefore that the observed cuspate–lobate traces and scaling relationship between amplitude and chord length of the lobes cannot be explained by post-thrusting buckling of the thrust surfaces. Moreover, the theory of buckling of competent layers or multilayers embedded in incompetent matrix and subsequent modification in fold geometry by flattening (Ramsay, 1967; Ramsay and Huber, 1987; Ghosh, 1993) indicates that a general wavelength–amplitude scaling of symmetric folds is unlikely, and has not been reported so far.

Topographic effects could in theory modify the smooth antiformal and synformal closures of wavy thrust traces into cuspate–lobate shapes. On traces of hinterland-dipping thrusts, these modifications will develop best if the topographic valleys occur along the antiformal axial zones and slope opposite to the plunge of the fold axes. Such a relationship consistently along the entire stretch of the Himalaya is unlikely. Moreover, as mentioned earlier, many of the cusps do not occur along the valleys. So the possibility of formation of the cuspate–lobate pattern by combination of post-thrusting folding and topographic undulations can be ruled out.

(3) An older upper level thrust surface may be passively folded because of displacement along a younger thrust at a lower level (e.g. Boyer and Elliott, 1982). Axes of the folds will be at low angles or even subparallel to the thrust transport, if the lower level thrust is cutting up as a lateral ramp. There is no evidence of such ramps below the thrusts showing cuspate–lobate trace (Fig. 1). Moreover, the lateral ramp model cannot explain the linear relationship between L and A. So, the possibility of formation of the cuspate–obate trace pattern by passive folding of thrusts due to displacement along a lower thrust can also be ruled out.

3.3. Differential transport

According to the model of fault growth proposed by Elliott (1976), a fault surface grows in all directions from an initial break at a point, which is the nucleus. The central part of a fault, which is also its oldest part, starts moving first compared with the lateral parts that start moving later as and when the fault rupture spreads laterally. As a result displacement varies within a fault (Elliott, 1976; Coward and Potts, 1983; Ellis and Dunlap, 1988). On surface-rupturing thrusts, the displacement variation leads to differential transport at the leading edge, which, as a consequence, will be curved. Subsequent slip accumulation by ground rupturing slip in the same or adjacent areas may enhance the leading edge curvature. Erosion or sediment burial may modify the geometry of the curved leading edges.

The preceding discussion shows that surface rupturing thrust sheets moving on planar thrusts may have a curved leading edge. Removal of the leading edge by deep erosion, however, will give a straight-line trace of the faults on an even topographic surface. Moreover, the tip line (Elliott, 1976; Coward and Potts, 1983) of blind faults typically forms a closed loop, which lies on the fault surface. If the fault surface is planar, its subsequent exhumation will also give a straight-line trace on an even topographic surface. We find, therefore, that differential transport on planar thrusts cannot explain the curved trace of deeply eroded surface-rupturing thrusts, or blind and subsequently exhumed thrusts. Long segments of the MCT, Shumar and Jutogh/Kulu thrusts sampled for the present study (Fig. 1) have Precambrian rocks on both sides of their

traces. Absence of synorogenic rocks of the Mesozoic–Tertiary Himalayan orogeny at the footwall of the thrusts indicates removal of the footwall synorogenic rocks by deep erosion, or these are exhumed blind thrusts on which the Precambrian sheets moved but did not rupture the surface to spread on synorogenic surfaces. As mentioned earlier, in both these situations differential transport on planar faults cannot generate the observed curved trace.

4. Fault growth along laterally curved surfaces

A thrust surface may be curved due to growth along laterally curved trajectories (Fig. 6; Ray, 1995, fig. 10). As a result, map trace of the thrust surface will also be curved. The curvatures in the dip direction will not significantly affect the trace pattern. According to this model of thrust fault growth, the fault segments, each growing along concave-upward laterally curved trajectories, coalesce to form large thrust surfaces. The lateral curvature gives a furrow-like shape to each segment, which are joined along sharp angular ridges. As a consequence, the thrust surface acquires a ridge-and-furrow shape, which is reflected in the cuspate–lobate trace pattern (Ray, 1995). This model of thrust fault growth can explain the multiple-lobate trace pattern of the sampled thrusts in the Lesser Himalaya (Fig. 1).

Lateral ramps, or 'hard' segment linkages (see Kim and Sanderson (2005) for a review) that establish segment connectivity by faults breaching the relay zones, may also generate laterally curved thrust surfaces. The surfaces will have long planar flats connected by short and curved ramps or jogs/bends. The traces will be curved only at the ramps or jogs/bends, and straight in the remaining parts. The sampled cuspate–lobate traces (Fig. 1) on the contrary, have smoothly rounded lobes separated by sharply curved cusps. Moreover, as mentioned earlier, a lateral ramp model cannot explain the linear relationship of L and A.

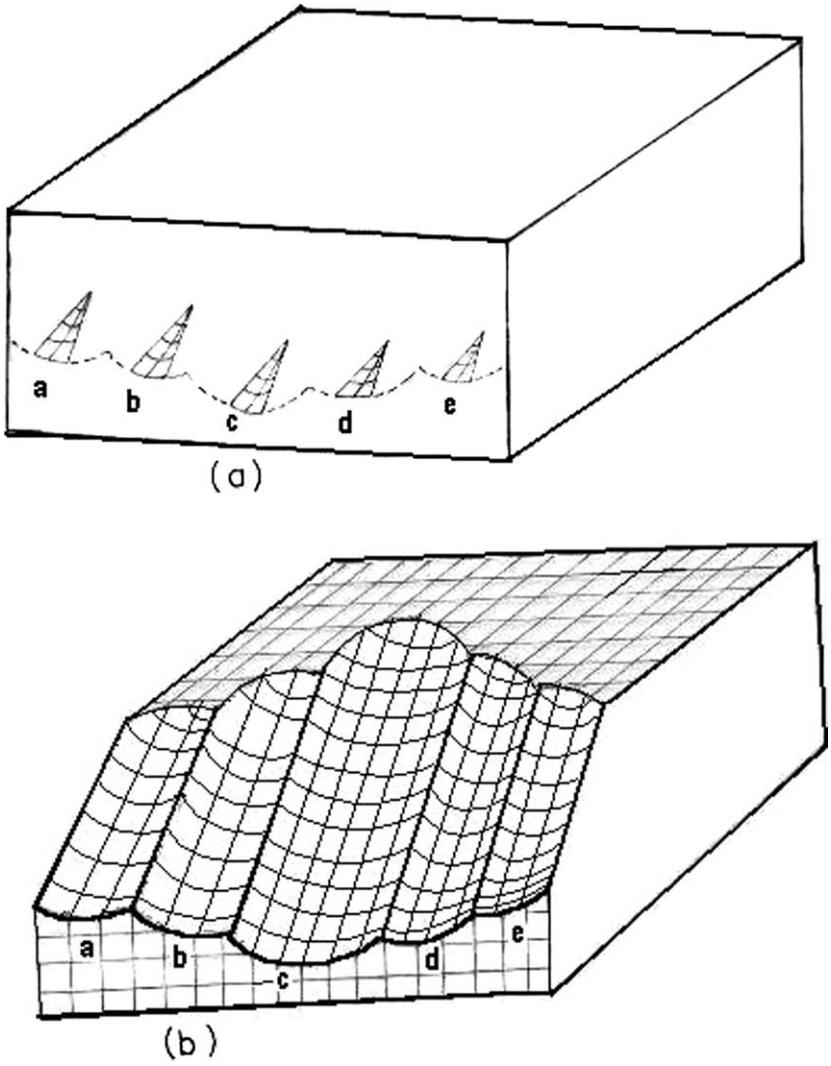

Fig. 6. Schematic representation of fault growth from multiple nuclei along laterally curved surfaces. (a) Early stage of growth from multiple nuclei a–e. The ruptures have started growing from each nucleus along concave-upward lateral trajectories. (b) Segments growing from each of the nuclei have coalesced by lateral linkage to form the thrust surfaces. The coalesced thrust surface has a fluted or ridge-and-furrow appearance, which gives rise to the cuspate–lobate map trace pattern of the thrust. Note that the curvature in the dip direction will have no effect on trace on a flat topographic surface.

5. Inferences on thrust fault growth

The cuspate–lobate trace pattern of the thrust faults in the Himalaya reflects the ridge-and-furrow, or fluted geometry of the thrust surfaces. Growth of such a fluted thrust surface can be explained by the model (Fig. 6) discussed in the preceding section. The model envisages growth of thrust segments from multiple nuclei, along concave-upward laterally curved trajectories. The trace pattern, however, does not lend support to the listric curvature (in the dip direction) of the flutings shown by Ray (1995, fig. 10).

Any ridge at high angle to the direction of transport will tend to act as an asperity barrier and will lead to either fault-bend folding, or removal of the asperity forming fault slivers or 'horses'. Ridges parallel to the transport direction will, however, tend to be preserved and may influence subsequent distributions of displacement as some parts of the fault surface will be more ideally oriented for slip compared with others.

The conventional models of fault growth envisage segment growth along planar surfaces. The nuclei of the segments do not lie on a plane, and so the propagating tips approach but cannot join one another. Connectivity in lateral direction is established by lateral ramps, or by faults that breach the relay zones ('hard' segment linkages; Kim and Sanderson, 2005). Segment linkage, however, is automatically established in faults growing along laterally curved trajectories. The trajectories should eventually meet even if the propagating surface of one segment passes by the advancing tip of the adjacent segment (Fig. 7). The lateral tips of the segments may continue to propagate through the thrust sheet as intersecting faults (Fig. 7b), or lateral propagation of the tips may stop after the segments coalesce (Fig. 7c). Further field observation and research is needed to test the possibilities. The traces of the sampled thrusts (Fig. 1), however, support that lateral propagation stops after the segments coalesce.

This model can also explain the linear scaling property of the lobes if we assume that growth of fault segments from their respective nuclei follow a particular curve (Fig. 4). Further research is required to test the validity of this assumption.

Fault surfaces are rarely uniformly smooth in mesoscopic scale. Instead, they are ornamented by different tectonic features ranging from millimeter to decameter scales. Striation grooves oriented parallel to slip direction are common features on fault surfaces. Stewart and Hancock (1991) reported fault surface corrugations ranging in scale from ripple-like features to several meters in amplitude and wavelength. The examples presented here reveal macroscopic scale thrust surface undulations of amplitudes on kilometer scales. Combining

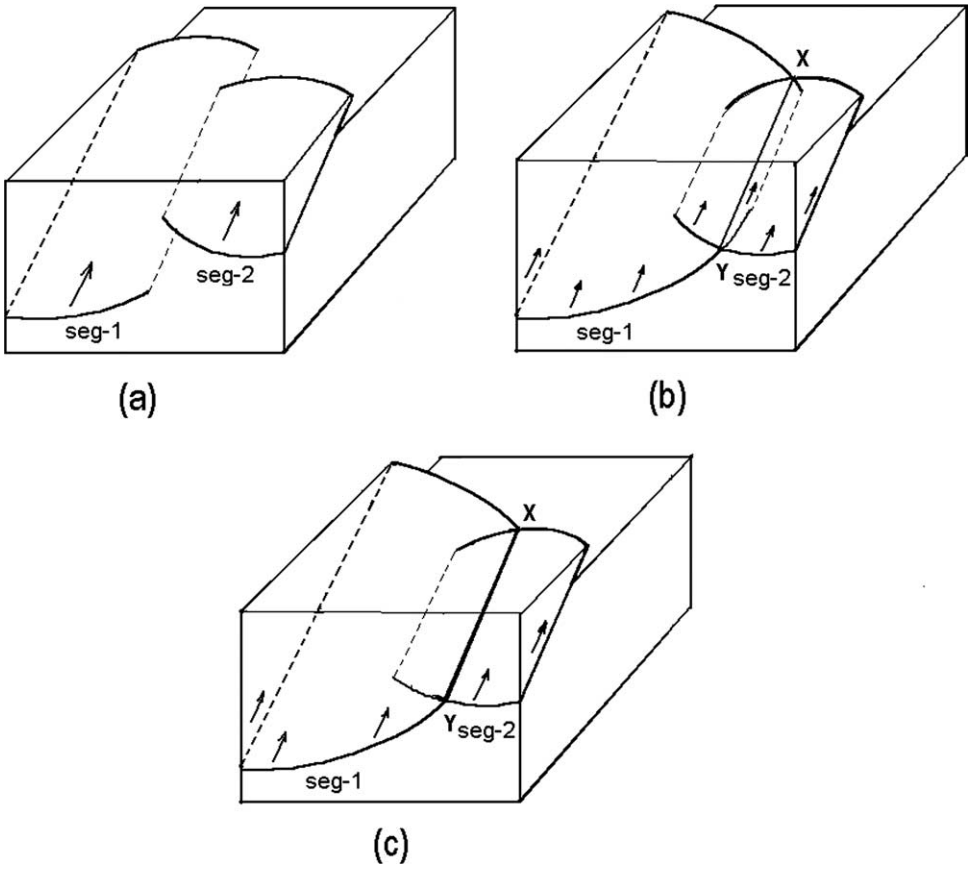

Fig. 7. Schematic diagram illustrating linkage of thrust fault segments propagating along concave-upward laterally curved surfaces. (a) Seg-1 and Seg-2 are two thrust fault segments propagating along concave-upward laterally curved trajectories. The upper level thrust (Seg-2) has passed by the propagating lateral tip of the Seg-1. (b) The two segments have coalesced along the line XY. After linkage is established, the lateral tips of Seg-1 and Seg-2 have continued to propagate through the thrust sheet. (c) The two segments have coalesced along the line XY. Further lateral propagation of the tips has stopped after segment linkage. Parts (b) and (c) represent two separate models of post-linkage growth. Field evidence supports (see text) the model (c).

these observations we may infer the possibility that thrust surfaces are fluted in a continuum of size scale ranging from millimeter scale striation grooves to kilometer scale flutings, oriented parallel to thrust movement direction.

6. Conclusions

A study of map traces of large thrust faults from different sectors of the Lesser Himalaya shows that the traces have a conspicuous cuspate–lobate pattern. The chord-length (L) and amplitude (A) of the lobes have an approximately linear scaling property that can be expressed by the equation $A = cL$, where c is a constant. The L and A values of the lobes on the sampled segments of the thrust traces show that the L/A ratio remains almost constant, over about a 1.71 order of magnitude spread of the L values. Topographic undulations, post-thrusting folding or differential transport along faults cannot explain the observed pattern and the scaling property of the thrust traces.

The pattern reflects laterally curved and fluted fault surfaces, which are inferred to be a primary feature related to thrust fault growth. The feature develops as the fault segments grow from their respective nuclei, along concave-upward laterally curved surfaces. This lateral curvature gives a furrow-like shape to the segments. Segment linkage is automatically achieved, because the propagating surfaces of the segments must eventually meet because of their curved trajectories. Several such segments, growing from multiple nuclei, coalesce along sharp angular ridges to form a large thrust surface, which has a fluted shape. The cuspate–lobate trace pattern is a result of the flutings on thrust surfaces. The pattern supports the possibility first indicated by Anderson (1951, p. 17) that fault surfaces have a fluted appearance, with fluting in the movement direction.

Millimeter-scale striation grooves parallel to movement direction, ripple size to decameter scale corrugations on normal faults (Stewart and Hancock, 1991) and the kilometer-scale undulations reported in this paper together suggest the possibility that thrust surfaces are rarely uniformly smooth, and are corrugated in a continuum of size scale ranging from millimeters to kilometers. The self-similarity of the lobes on the fault traces indicates the possibility that thrust fault surfaces grow along a particular curved surface, which is the characteristic surface of thrust fault propagation. Further research is needed to test the possibilities.

Acknowledgements

Facilities to carry out this research were provided by the Geological Survey of India. I thank D.J. Sanderson and David Peacock for helpful reviews. D.J. Sanderson provided many suggestions that encouraged and helped the author to revise and improve the paper. I also thank JSG Editor R.E. Holdsworth for his comments and help in improvement of the paper.

References

Ahmad, A., 1979. Facies concept, correlation and classification of Palaeozoic (pre-Blaini) formations of Kumaun, Gahwal and Himachal Lesser Himalaya, India. Geological Survey of India Miscellaneous Publication 41 (Part I), 209–240.

Anderson, E.M., 1951. The Dynamics of Faulting, 2nd ed Oliver and Boyd, Edinburgh, U.K..

Armijo, R., Tapponier, P., Mercier, J.L., Tong-Lin, H., 1986. Quaternary extension in southern Tibet: field observations and tectonic implications. Journal of Geophysical Research 91, 13803–13872.

Boyer, S.E., Elliott, D., 1982. Thrust systems. American Association of Petroleum Geologists Bulletin 66, 1196–1230.

Coward, M.P., Potts, G.J., 1983. Complex strain patterns developed at the frontal and lateral tips to shear zones and thrust zones. Journal of Structural Geology 5, 383–399.

Elliott, D., 1976. The energy balance and deformation mechanisms of thrust sheets. Philosophical Transactions of the Royal Society London Series A 263, 289–312.

Ellis, M.A., Dunlap, W.J., 1988. Displacement variation along thrust faults: implications for the development of large faults. Journal of Structural Geology 10, 183–192.

Geological Survey of India, 1989.Anon., 1989. Geology and Tectonics of the Himalaya. Geological Survey of India, Special Publication 26, Calcutta.

Ghosh, S.K., 1993. Structural Geology: Fundamentals and Modern Developments. Pergamon Press, Oxford.

Jangpangi, B.S., 1982. Structure and tectonics of the crystalline rocks of Central Himalaya (Kumaon and Garhwal). Geological Survey of India Miscellaneous Publication 41 (Part III), 133–148.

Kim, Y.-S., Sanderson, D.J., 2005. The relationship between displacement and length of faults: a review. Earth-Science Reviews 68, 317–334.

Kizaki, K., Ohta, Y., Arita, K., 1982. Structure of the Midland Metasediments Group of Central East Nepal. Geological Survey of India Miscellaneous Publication 41 (Part III), 271–275.

Kumar, G., 1997. Geology of Arunachal Pradesh. Geological Society of India, Bangalore.

Le Pichon, X., Fournier, M., Jolivet, L., 1992. Kinematics, topography, shortening, and extrusion in the India–Eurasia collision. Tectonics 11, 1085–1098.

Macedo, J., Marshak, S., 1999. Controls on the geometry of fold-thrust belt salients. Geological Society of America Bulletin 111, 1808–1822.

Nanda, A.C., Mathur, A.K., 2000. Palaeogeographic and Palaeoecologic Evolution of Paratethyan Basins during Neogene and their Correlation to Global Scales, IGCP Project-329, Miscellaneous Publication No. 64. Geological Survey of India, Calcutta.

Ramsay, J.G., 1967. Folding and Fracturing of Rocks. McGraw-Hill, London.

Ramsay, J.G., Huber, M.I., 1987. The Techniques of Modern Structural Geology, Vol. 2: Folds and Fractures. Academic Press, London.

Ray, S.K., 1991. Significance of forelimb folds in the Shumar allochthon, Lesser Himalayas, eastern Bhutan. Journal of Structural Geology 13, 411–418.

Ray, S.K., 1995. Lateral variation in geometry of thrust planes and its significance, as studied in the Shumar allochthon, Lesser Himalayas, eastern Bhutan. Tectonophysics 249, 125–139.

Ray, S.K., 2000. Culmination zones in eastern Himalaya. Geological Survey of India, Special Publication 55, 85–94.

Ray, S.K., Bandyopadhyay, B.K., Razdan, R.K., 1989. Tectonics of a part of the Shumar allochthon in eastern Bhutan. Tectonophysics 169, 51–58.

Seeber, L., Gornitz, V., 1983. River profiles along the Himalayan arc as indicators of active tectonics. Tectonophysics 92, 335–367.

Sharma, R.P., Virdi, N.S., 1982. Tectonic evolution of Simla and Kumaon Himalaya, based on Landsat-I multispectral imagery and aerial photo-interpretation. Geological Survey of India Miscellaneous Publication 41 (Part III), 115–132.

Sharma, V.P., 1977. Geology of the Kulu–Rampur belt, Himachal Pradesh. Memoirs of the Geological Survey of India 106 (Part II), 235–407.

Srikantia, S.V., Bhargava, O.N., 1998. Geology of Himachal Pradesh. Geological Society of India, Bangalore.

Stewart, I.S., Hancock, P.L., 1991. Scale of structural heterogeneity within neotectonic normal fault zones in the Aegean region. Journal of Structural Geology 13, 191–204.